Consistency of patterns in concentration-discharge plots

Jeffrey G. Chanat
Department of Environmental Sciences, University of Virginia, Charlottesville, Virginia, USA

Karen C. Rice
U.S. Geological Survey, Charlottesville, Virginia, USA

George M. Hornberger
Department of Environmental Sciences, University of Virginia, Charlottesville, Virginia, USA

Received 27 September 2001; revised 12 March 2002; accepted 28 March 2002; published 17 August 2002.

[1] Concentration-discharge (c-Q) plots have been used to infer how flow components such as event water, soil water, and groundwater mix to produce the observed episodic hydrochemical response of small catchments. Because c-Q plots are based only on observed streamflow and solute concentration, their interpretation requires assumptions about the relative volume, hydrograph timing, and solute concentration of the streamflow end-members. *Evans and Davies* [1998] present a taxonomy of c-Q loops resulting from three-component conservative mixing. Their analysis, based on a fixed template of end-member hydrograph volume, timing, and concentration, suggests a unique relationship between c-Q loop form and the rank order of end-member concentrations. Many catchments exhibit variability in component contributions to storm flow in response to antecedent conditions or rainfall characteristics, but the effects of such variation on c-Q relationships have not been studied systematically. Starting with a ''baseline'' condition similar to that assumed by *Evans and Davies* [1998], we use a simple computer model to characterize the variability in c-Q plot patterns resulting from variation in end-member volume, timing, and solute concentration. Variability in these three factors can result in more than one c-Q loop shape for a given rank order of end-member solute concentrations. The number of resulting hysteresis patterns and their relative frequency depends on the rank order of solute concentrations and on their separation in absolute value. In ambiguous cases the c-Q loop shape is determined by the relative ''prominence'' of the event water versus soil water components. This ''prominence'' is broadly defined as a capacity to influence the total streamflow concentration and may result from a combination of end-member volume, timing, or concentration. The modeling results indicate that plausible hydrological variability in field situations can confound the interpretation of c-Q plots, even when fundamental end-member mixing assumptions are satisfied. *INDEX TERMS:* 1806 Hydrology: Chemistry of fresh water; 1860 Hydrology: Runoff and streamflow; 1871 Hydrology: Surface water quality ; *KEYWORDS:* episodic hydrochemistry, concentration-discharge relationships, mixing models

1. Introduction

[2] Concentration-discharge (c-Q) plots are a convenient and increasingly popular tool for interpreting the episodic hydrochemical response of small forested basins [e.g., *Buttle and Peters*, 1997; *Evans and Davies*, 1998; *Biron et al.*, 1999; *Evans et al.*, 1999; *Scanlon et al.*, 2001; *Hornberger et al.*, 2001]. Construction of c-Q plots requires only data on streamflow and stream chemistry at the catchment outlet [*Evans and Davies*, 1998]. The plots typically exhibit looping patterns, which range from simple, readily identifiable loops to more complex indeterminate shapes. These patterns can be used to infer runoff processes and pathways, augmenting or potentially substituting for hydrometric measurements [*Evans and Davies*, 1998] or more elaborate mathematical techniques [*Hornberger et al.*, 2001]. Interpretations are dependent on an underlying conceptual model of catchment behavior, however, and must be made with knowledge of what patterns are consistent with a given model.

[3] *Evans and Davies* [1998] provide an excellent review of the literature on relationships between solute concentration and stream discharge, and suggest a taxonomy for the simpler loops based on component mixing models. The specific assumptions of mixing models vary between studies, but the most general assumptions are (1) streamflow is the sum of component flows from a fixed number of end-members, (2) water resident in or passing through any end-member acquires a chemical or isotopic signature that distinctly characterizes that end-member, (3) the signatures are all time-invariant, and (4) the components do not mix until they reach the stream.

0043-1397/02/2001WR000971$09.00

[4] In most studies, either two or three components are considered. In two-component models [e.g., *Buttle*, 1994], the components are usually identified as "old" and "new" water, reflecting an emphasis on the time of origin. In three-component studies [e.g., *DeWalle et al.*, 1988], the components are often broadly classified as groundwater, soil water, and event water, reflecting an emphasis on the geographic source. In this study, we use the term "event water" to refer to that which reaches the stream channel without ever infiltrating the soil surface. The signature of the groundwater component, or the "old" water in the two-component case, is often approximated by the solute concentration in base flow.

[5] For a three-component model, the mass balance equation for a single solute is:

$$Q_T C_T = Q_G C_G + Q_S C_S + Q_E C_E, \quad (1)$$

where Q is discharge, C is concentration, and the subscripts G, S, E, and T refer to groundwater, soil water, event water, and total water, respectively. If the general mixing assumptions are satisfied, the solute concentration in the stream at any point in time depends entirely on the volumetric component contributions and their solute concentrations. The trajectory of the c-Q trace over the course of a storm is thus determined by 1) the relative component volumes, or "size" of the component hydrographs, 2) the shape and timing of the component hydrographs, and 3) the solute concentrations in the end-members. In principle, if any two of these factors are known, the characteristics of an observed c-Q trace can be used to infer the third. In their model, *Evans and Davies* [1998] assume a generic three-component hydrograph template, effectively fixing factors one and two. Their template, based on processes thought "likely to operate widely in humid forested basins", consists of an early peak in event water, a groundwater peak coincident with peak storm flow, and a later soil water peak. The authors suggest that under these constraints, any relative rank of end-member solute concentrations is uniquely associated with a characteristic looping pattern in the c-Q plot. They define six generic loop shapes, associated with the six possible permutations of end-member concentrations. These loops are named C1-C3 and A1-A3, where "C" or "A" refer to clockwise or anticlockwise rotation, and 1-3 refer to whether the loop has lobes both above and below, strictly above, or strictly below the base flow concentration, respectively [*Evans and Davies*, 1998] (Figure 1). The authors further suggest that the unique relationship between c-Q loop shape and end-member concentration is robust to variation in absolute end-member concentration and component discharge magnitude. They cite changes in the relative time order of the hydrograph peaks as a factor that may invalidate their taxonomy, and caution against applying the classification in regions where the time order is known to differ from the assumed template [*Evans and Davies*, 1998].

[6] Even in humid forested catchments where the proposed template may apply, variability in hydrograph component volume and timing, often in response to antecedent conditions or rainfall characteristics, is frequently significant. *Swistock et al.* [1989] report typical storm volume ratios for event, soil, and groundwater of 5, 20, and 75%, respectively, on a small Pennsylvania stream. These ratios are generally consistent with the hydrograph template used by *Evans and Davies* [1998]. However, *Swistock et al.* [1989] measured event water contributions of up to 38% for intense storms on dry antecedent conditions, and observed that the soil water peak could advance to coincide with or even precede the groundwater peak for storms on wet antecedent conditions. *DeWalle et al.* [1988] reported similar typical volume ratios for the same catchment, but noted soil water contributions as high as 40% for rainfall on wet soil. Typical component hydrograph timing was broadly consistent with the template used by *Evans and Davies* [1998]. *Bazemore et al.* [1994] reported similar variability on a steep headwater catchment in the Virginia Blue Ridge, noting increased soil- and event water volume, and a peak flow dominated by soil water, for larger storms.

[7] Uncertainty in end-member solute concentration is an additional potential source of variability in c-Q plot shape. It is notoriously difficult to characterize the "effective" end-member concentrations in spatially variable soil reservoirs [e.g., *McDonnell et al.*, 1991] or temporally variable rainfall fields [e.g., *McDonnell et al.*, 1990; *Pionke and DeWalle*, 1992].

[8] Our central hypothesis is that plausible perturbations in the component hydrograph volumes, the component hydrograph timing, and the end-member concentrations, none of which may be detectable without extensive field instrumentation, can complicate the interpretation of c-Q plots and potentially undermine their diagnostic power. In this study, we investigate the effects of variability in component hydrograph characteristics and end-member solute concentrations on the patterns of three-component c-Q plots generated by conservative mixing processes. We construct a simple computer model that displays the c-Q plot resulting from the arrangement of three component hydrograph "building blocks" and a given set of end-member concentrations. Then, beginning with a physically reasonable "baseline" condition similar to that used by *Evans and Davies* [1998], we apply the model to explore the range of possible c-Q plot patterns that might arise when the hydrograph volume, hydrograph timing, and end-member concentrations are allowed to vary. Results indicate that under some circumstances the pattern of a c-Q loop is not unambiguously determined by the rank order of concentrations of end-members, even when the simple mixing assumptions are met.

2. Methods

[9] The overall experimental approach involved 1) generating a large number of synthetic c-Q plots with different end-member hydrographs and solute concentrations, 2) classifying the plots according to looping pattern, and 3) identifying the conditions under which a given set of general circumstances resulted in more than one type of plot.

[10] The plot generation mechanism was a simple computer implementation of the conservative three-component mixing relationship. A set of three triangular hydrographs was created to represent event water, soil water, and groundwater components. Each had unit volume, in arbitrary units, and a risetime equal to one-half the recession time. The event water component had a time base of 19 arbitrary time units;

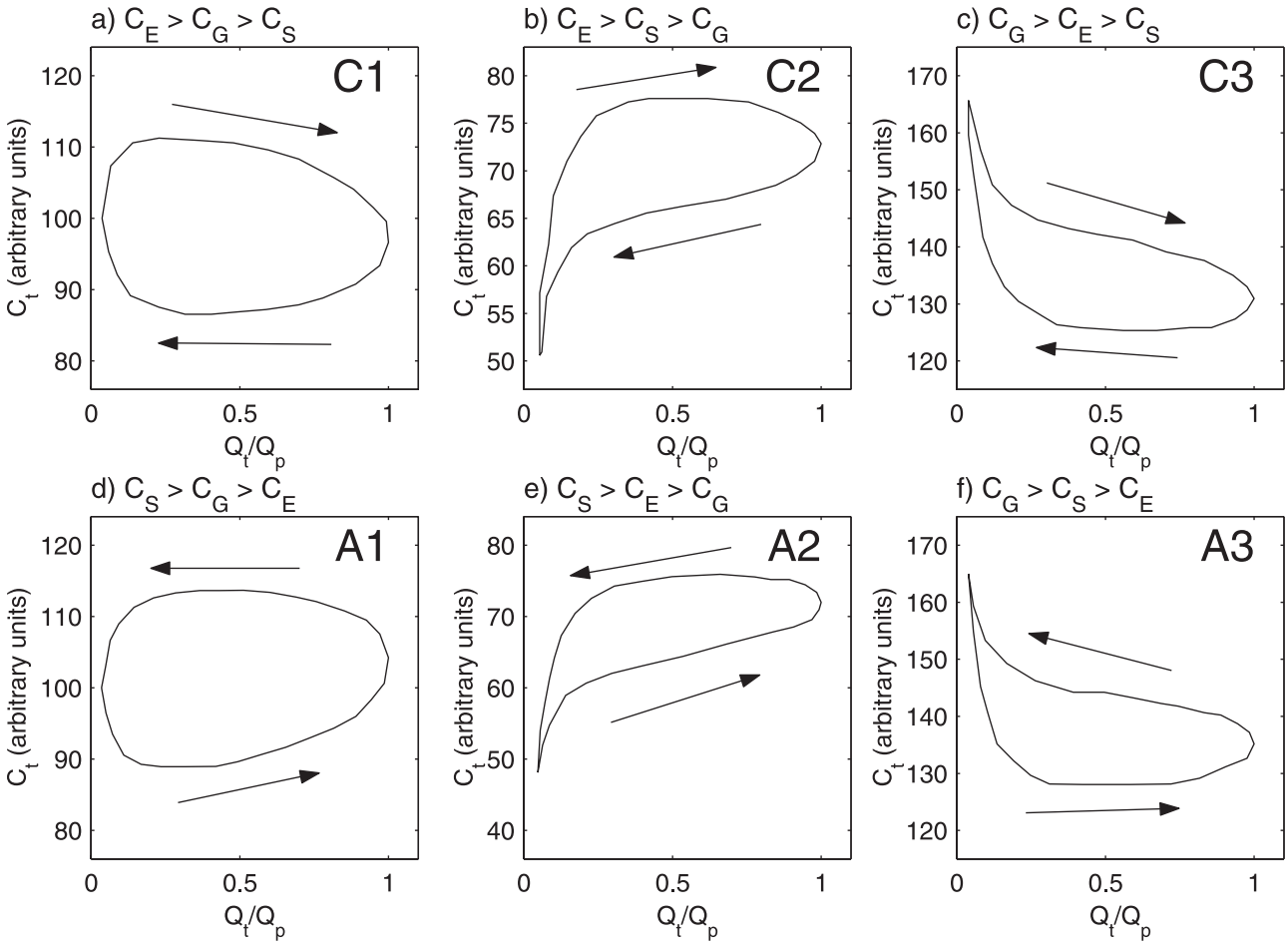

Figure 1. Example concentration-discharge (c-Q) loops illustrating the taxonomic scheme of *Evans and Davies* [1998]. Arrows indicate direction of rotation. C represents concentration; Q represents discharge. Subscripts E, S, G, T, and P represent event water, soil water, groundwater, total flow, and peak flow, respectively. Refer to text for description of loop identifiers. After *Evans and Davies* [1998].

the soil- and groundwater components had time bases of 28 and 37 units, respectively. Each of the three component hydrographs was multiplied by a volume scaling factor, and each was associated with a concentration of a generic conservative solute. The three hydrographs were superimposed on a constant base flow of 0.1 arbitrary flow units, with the order of their peaks constrained to event water—groundwater—soil water (Figure 2). Given values for the parameters defining the hydrographs and the component concentrations (Figure 2), the total flow volume and concentration time series can be computed by use of equation (1).

[11] A set of baseline volume, timing, and concentration parameters was chosen to represent the typical, or ''mean'' condition. The baseline volume scaling factor for the groundwater component was chosen such that the peak groundwater storm flow was ten times the base flow, or 1.0 units. Baseline volume scaling factors for event and soil water were then chosen such that event, soil, and groundwater contributed 5, 20, and 75% of total storm flow, respectively, consistent with the results reported by *Swistock et al.* [1989]. Under these constraints, the baseline ratio of V_E:V_S:V_G is 1.2:4.9:18.5. The baseline timing was similar to that used by *Evans and Davies* [1998], with an event water peak early in the storm (t = 10), a groundwater peak coincident with peak storm discharge (t = 16), and a later soil water peak (t = 22). Two ranges of baseline solute concentrations were defined: a ''narrow'' range with concentrations of 50, 100, and 150 arbitrary units, and a ''broad'' range with concentrations of 10, 100, and 1000 units. The three concentration values could be assigned to the event water, soil water, and groundwater end-members in any of six permutations. The base flow component was assigned the same solute concentration as the groundwater.

[12] Eight model parameters (V_E, V_S, V_G, T_E, T_S, C_E, C_S, C_G) were varied around the baseline case in a set of three Monte Carlo experiments (Table 1). Parameters were sampled from independent uniform distributions. Ranges for the parameters were selected to broadly reflect conditions reported by *Swistock et al.* [1989] and *Bazemore et al.* [1994]. The volume scaling factors for event water, soil water, and groundwater were varied independently on the intervals (0.2–2.2), (2.9–6.9), and (15.5–21.5), respectively. With this arrangement, the maximum and minimum contributions of event water, soil water, and groundwater to total storm flow in independent realizations were 1–10, 12–28, and 65–86%, respectively.

[13] The timing of the event water peak was allowed to vary on the interval (7–13), and the soil water peak

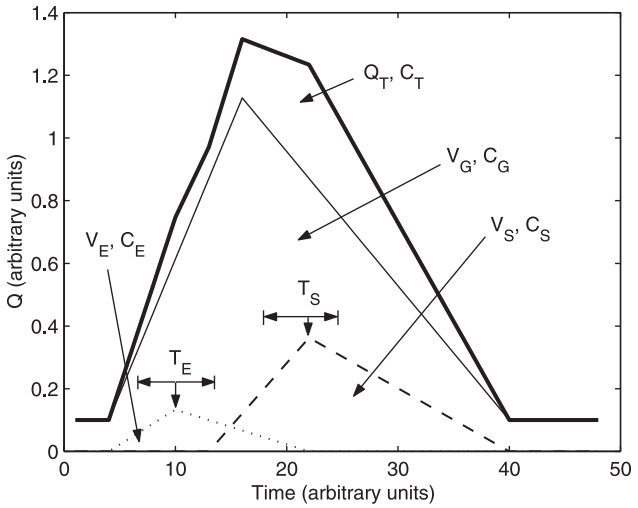

Figure 2. Component hydrograph layout and parameters used in the three Monte Carlo experiments. Dotted line represents event water, dashed line represents soil water, solid line represents groundwater, and thick solid line represents total flow. Q, C, V, and T represent discharge, concentration, volume, and time, respectively. Subscripts E, S, G, and T represent event water, soil water, groundwater, and total flow, respectively.

independently on the interval (18–24), while the groundwater peak time was held constant at t = 16. In approximately 10% of the realizations, the combination of timing and volume produced double-peaked composite hydrographs. In natural systems, a double-peaked hydrograph resulting from a single rainfall input may in itself suggest the dominant runoff mechanisms. Because the intent of this investigation is to examine the strength of inferences about runoff processes based solely on the c-Q plot, realizations that produced this additional "clue" were discarded.

[14] Concentrations were varied in nonoverlapping intervals. When the narrow concentration range was used, the intervals were (25–75), (75–125), and (125–175) units; when the broad range was used, the intervals were (5–15), (50–150), and (500–1500) units.

[15] The first experiment was designed to explore the robustness of a single loop type under a restricted range of variability in environmental factors. Only the component volume scaling factors were varied (Table 1, experiment 1). Timing was fixed at the mean values, and mean values from the narrow concentration range were applied to end-member concentrations in the ranking $C_G > C_S > C_E$. One hundred single-peaked realizations were generated. The second experiment was a more general evaluation of the sensitivity of all loop types to simultaneous variation in timing, volume, and concentration (Table 1, experiment 2). Here, a total of six separate simulations were conducted, with concentration values from the narrow range assigned to the end-members in all six possible permutations. For each of the six simulations, 500 realizations were generated. The third experiment was designed to evaluate the effect of absolute differences in concentration on the robustness of all six loop types. This experiment was identical to the second, except the narrow concentration range was replaced with the broad range (Table 1, experiment 3).

[16] The c-Q plots were classified as C1-C3 and A1-A3 following the scheme of *Evans and Davies* [1998]. The concentration values at flows corresponding to 25, 50, and 75% of the peak flow on both the rising and receding limb were recorded. Plots where all three rising limb concentrations were greater than the corresponding receding limb values were classified as "C" (clockwise); those for which the reverse was true were classified as "A" (anticlockwise). Any plot that did not satisfy either criterion was assigned to a separate "indeterminate" category. For "C" and "A" loops, the numeric portion of the classification was assigned based on comparing the entire set of concentration values to the base flow concentration. If the loop contained points both above and below base flow concentration, the numeric portion was set to "1". If all the points were greater than or equal to base flow concentration, the numeric portion was set to "2", and if all the points were less than or equal to base flow concentration, the numeric portion was set to "3". The distribution of loop types resulting from each simulation was tabulated, and the results compared to the loop type expected in the "static" scenario described by *Evans and Davies* [1998]. For the first experiment, the ranking $C_G > C_S > C_E$ is expected to produce an A3 loop; each of the six rankings in experiments 2 and 3 is expected to produce a unique corresponding loop shape (Figure 1).

[17] To determine the factors most closely associated with different c-Q patterns, the classes of curves resulting from each simulation were used as groups in a discriminant function analysis (DFA). Discriminant functions were selected using a stepwise method, with alpha value criteria of 0.05 to include a predictor in the model and 0.10 to retain it. In the first experiment, the three component volume scaling factors were the only possible candidate predictors. The second and third experiments had a total of eight candidate predictors: the three volume scaling factors, the time of the event and soil water peaks, and the concentrations in the three end-members.

3. Results

3.1. Experiment 1

[18] Of the 100 c-Q loops generated in the first experiment, only 24 were classified as the expected A3 pattern. Thirty loops were classified as C3, and 46, or just under half, were indeterminate (Table 2, experiment 1). The first standardized discriminant function explained nearly all of the total dispersion of the group centroids (Figure 3). In all cases where DFA was applied in this investigation, the first discriminant function explained 95% or more of the total dispersion; only the first function will be discussed hereafter. The function had more positive values when the event water volume scaling factor was high and the soil water volume scaling factor was low (Table 2, experiment 1). The groundwater volume scaling factor was not among the heavily weighted predictors in any of the three experiments. High values of the discriminant function were associated with A3 rotation, low values with C3 rotation, and intermediate values with indeterminate rotation (Figure 3).

3.2. Experiment 2

[19] Loop types C1 and A1, associated with concentration ranks $C_E > C_G > C_S$ and $C_S > C_G > C_E$, respectively,

Table 1. Concentration Rankings and Parameters Used in the Three Monte Carlo Experiments[a]

Concentration Rank	Volume Scaling Factor			Peak Time (Arbitrary Units)			Concentration (Arbitrary Units)			Number of Realizations
	Event Water (V_E)	Soil Water (V_S)	Groundwater (V_G)	Event Water (T_E)	Soil Water (T_S)	Groundwater (T_G)	Event Water (C_E)	Soil Water (C_S)	Groundwater (C_G)	
Experiment 1[b]										
$C_G > C_S > C_E$	1.2 (0.2–2.2)	4.9 (2.9–6.9)	18.5 (15.5–21.5)	10	22	16	50	100	150	100
Experiment 2[c]										
$C_E > C_G > C_S$	1.2 (0.2–2.2)	4.9 (2.9–6.9)	18.5 (15.5–21.5)	10 (7–13)	21 (18–24)	16	150 (125–175)	50 (25–75)	100 (75–125)	500
$C_E > C_S > C_G$	1.2 (0.2–2.2)	4.9 (2.9–6.9)	18.5 (15.5–21.5)	10 (7–13)	21 (18–24)	16	150 (125–175)	100 (75–125)	50 (25–75)	500
$C_G > C_E > C_S$	1.2 (0.2–2.2)	4.9 (2.9–6.9)	18.5 (15.5–21.5)	10 (7–13)	21 (18–24)	16	100 (75–125)	50 (25–75)	150 (125–175)	500
$C_S > C_G > C_E$	1.2 (0.2–2.2)	4.9 (2.9–6.9)	18.5 (15.5–21.5)	10 (7–13)	21 (18–24)	16	50 (25–75)	150 (125–175)	100 (75–125)	500
$C_S > C_E > C_G$	1.2 (0.2–2.2)	4.9 (2.9–6.9)	18.5 (15.5–21.5)	10 (7–13)	21 (18–24)	16	100 (75–125)	150 (125–175)	50 (25–75)	500
$C_G > C_S > C_E$	1.2 (0.2–2.2)	4.9 (2.9–6.9)	18.5 (15.5–21.5)	10 (7–13)	21 (18–24)	16	50 (25–75)	100 (75–125)	150 (125–175)	500
Experiment 3[d]										
$C_E > C_G > C_S$	1.2 (0.2–2.2)	4.9 (2.9–6.9)	18.5 (15.5–21.5)	10 (7–13)	21 (18–24)	16	1000 (500–1500)	10 (5–15)	100 (50–150)	500
$C_E > C_S > C_G$	1.2 (0.2–2.2)	4.9 (2.9–6.9)	18.5 (15.5–21.5)	10 (7–13)	21 (18–24)	16	1000 (500–1500)	100 (50–150)	10 (5–15)	500
$C_G > C_E > C_S$	1.2 (0.2–2.2)	4.9 (2.9–6.9)	18.5 (15.5–21.5)	10 (7–13)	21 (18–24)	16	100 (50–150)	10 (5–15)	1000 (500–1500)	500
$C_S > C_G > C_E$	1.2 (0.2–2.2)	4.9 (2.9–6.9)	18.5 (15.5–21.5)	10 (7–13)	21 (18–24)	16	10 (5–15)	1000 (500–1500)	100 (50–150)	500
$C_S > C_E > C_G$	1.2 (0.2–2.2)	4.9 (2.9–6.9)	18.5 (15.5–21.5)	10 (7–13)	21 (18–24)	16	100 (50–150)	1000 (500–1500)	10 (5–15)	500
$C_G > C_S > C_E$	1.2 (0.2–2.2)	4.9 (2.9–6.9)	18.5 (15.5–21.5)	10 (7–13)	21 (18–24)	16	10 (5–15)	100 (50–150)	1000 (500–1500)	500

[a] Numbers outside parentheses indicate baseline values; numbers in parentheses indicate range of variation.
[b] Component hydrograph volume variable, hydrograph timing and end-member concentration fixed.
[c] Component hydrograph volume, timing, and end-member concentration variable; narrow concentration range.
[d] Component hydrograph volume, timing, and end-member concentration variable; broad concentration range.

Table 2. Distribution of Loop Types Observed in the Three Monte Carlo Experiments[a]

Concentration Rank	Expected Pattern	Observed Pattern							Discriminant Function	Prominent Component
		C1	C2	C3	A1	A2	A3	IND		
Experiment 1[b]										
$C_G > C_S > C_E$	A3			30			24	46	DF1: $1.15 * V_E - 0.78 * V_S$ DF2: $0.22 * V_E + 0.87 * V_S$	event water
Experiment 2[c]										
$C_E > C_G > C_S$	C1	500							n/a	n/a
$C_E > C_S > C_G$	C2		172			151		177	$1.03 * V_E - 0.79 * C_S - 0.75 * T_S$	event water
$C_G > C_E > C_S$	C3			445			1	54	$0.75 * T_E + 0.57 * T_S - 0.43 * V_E$	soil water
$C_S > C_G > C_E$	A1				500				n/a	n/a
$C_S > C_E > C_G$	A2		1			448		51	$0.65 * T_E - 0.58 * V_E + 0.55 * T_S$	soil water
$C_G > C_S > C_E$	A3			141			172	187	$0.97 * V_E + 0.70 * C_S - 0.66 * T_S$	event water
Experiment 3[d]										
$C_E > C_G > C_S$	C1	500							n/a	n/a
$C_E > C_S > C_G$	C2		420			8		72	$0.67 * V_E - 0.57 * T_E - 0.53 * T_S$	event water
$C_G > C_E > C_S$	C3			342			4	154	$0.91 * T_E + 0.71 * T_S - 0.69 * V_E$	soil water
$C_S > C_G > C_E$	A1				500				n/a	n/a
$C_S > C_E > C_G$	A2					500			n/a	n/a
$C_G > C_S > C_E$	A3			285			29	186	$0.85 * V_E - 0.81 * T_E - 0.69 * T_S$	event water

[a] Refer to text for explanation of discriminant functions and prominent components.
[b] Component hydrograph volume variable, hydrograph timing and end-member concentration fixed.
[c] Component hydrograph volume, timing, and end-member concentration variable; narrow concentration range.
[d] Component hydrograph volume, timing, and end-member concentration variable; broad concentration range.

were the only patterns that were 100% robust to perturbations in volume, timing, and concentration (Table 2, experiment 2). Loop type C3, associated with rank $C_G > C_E > C_S$, and loop type A2, associated with rank $C_S > C_E > C_G$, occurred in roughly 90% of the situations in which they were expected in the static scenario, with nearly all the exceptions being indeterminate. Loop types C2, associated with rank $C_E > C_S > C_G$, and A3, associated with rank $C_G > C_S > C_E$, occurred in only about one-third of the situations in which they were expected. Approximately half of the exceptions were indeterminate, and half showed reversed rotational direction.

[20] In the four cases that resulted in more than one loop type, five or six predictors were retained in the first discriminant function; only the three with the heaviest weighting are reported here. The signs of the discriminant function coefficients for these rankings have been adjusted so that a more positive value of the function is associated with the rotational pattern expected in the static scenario used by *Evans and Davies* [1998]. For concentration rankings $C_E > C_S > C_G$ and $C_G > C_S > C_E$, the discriminant function was positive when the event water volume was high, soil water concentration was close to the groundwater concentration, and the soil water peak was early, that is, close to the groundwater peak (Table 2, experiment 2). For rankings $C_G > C_E > C_S$ and $C_S > C_E > C_G$, the discriminant function was positive when the event water volume was low, the event water peak was late, that is, close to the groundwater peak, and the soil water peak was late, that is, distinct from the groundwater peak (Table 2, experiment 2).

3.3. Experiment 3

[21] Loop types C1 and A1, associated with concentration ranks $C_E > C_G > C_S$ and $C_S > C_G > C_E$, respectively, were again completely robust to variations in component volume, timing, and concentration (Table 1, experiment 3). Loop types C2, associated with ranking $C_E > C_S > C_G$, and A2, associated with ranking $C_S > C_E > C_G$, became more robust than in experiment 2, with loop type A2 becoming completely resilient to variability in physical conditions. In contrast, loop types C3 and A3, associated with rankings $C_G > C_E > C_S$ and $C_G > C_S > C_E$, respectively, became less robust. Only about 6% of the loops associated with concentration rank $C_G > C_S > C_E$ showed the expected A3

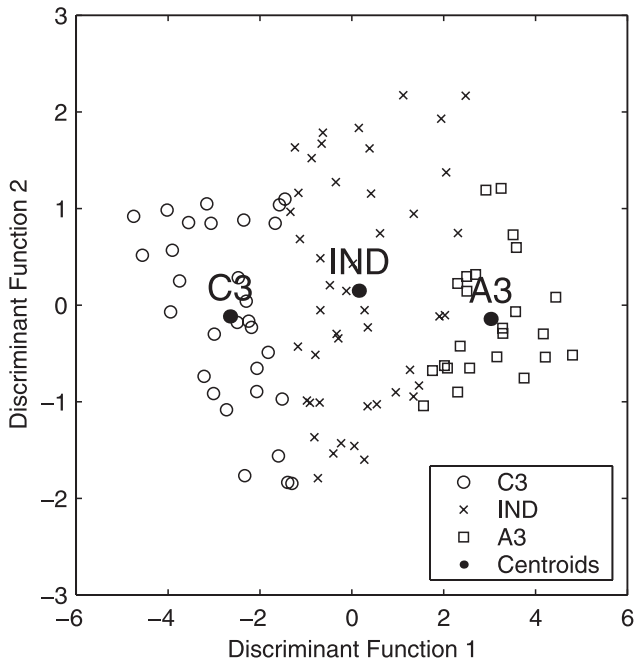

Figure 3. Results of the discriminant function analysis for experiment 1. Loop types C3 and A3 are separated primarily along the first discriminant function axis. Refer to Table 2 (experiment 1) for axis interpretations. IND represents indeterminate loop form.

pattern. Concentration parameters were no longer present in any of the discriminant functions. However, the most strongly weighted variables in each function were identical to those for the same concentration ranking in experiment 2.

4. Discussion

4.1. Experiment 1

[22] With hydrograph timing and concentration fixed, the first discriminant function in experiment 1 depends only on component volumes, taking more positive values when event water volume is in the upper end of its allowed range and soil water volume is in the lower end of its allowed range (Table 2, experiment 1). For convenience, when this condition is satisfied we refer to event water as the ''prominent'' component, even though event water is always a smaller volumetric proportion of the total hydrograph than soil water (Figure 2). Conversely, when the opposite condition is satisfied, we refer to soil water as the ''prominent'' component.

[23] The influence of event and soil water volume on c-Q loop rotational direction may be illustrated by selecting three sets of relative volumes representing a gradient from prominent event water to prominent soil water (Figure 4). Because the concentration ranking is $C_G > C_S > C_E$, all three loops dip down from, then return up to, the base flow value. When event water is prominent, the dilution due to event water on the rising limb is greater than that due to soil water on the receding limb. Thus the total concentration on the rising limb is consistently lower than that on the receding limb, and the ''expected'' A3 pattern results (Figure 4a). As the event water volume becomes smaller and soil water volume larger, the total concentrations increase along the rising limb and decrease along the receding limb. The result is a figure-eight-shaped indeterminate loop (Figure 4b). When soil water is prominent, dilution due to event water on the rising limb is smaller than that due to soil water on the receding limb, even though the event water concentration is lower than that of the soil water. Therefore the total concentration on the rising limb is everywhere higher than at the corresponding point on the receding limb, resulting in a C3 pattern (Figure 4c).

4.2. Experiment 2

[24] The complete robustness of loop types C1, associated with concentration rank $C_E > C_G > C_S$, and A1, associated with concentration rank $C_S > C_G > C_E$, is a direct result of the constraint on the sequence of the component peaks and the intermediate position of groundwater in the concentration ranking. With event water peaking before groundwater and soil water peaking afterwards, concentrations near the beginning of the storm result from mixing of only event and groundwater, and those near the end of the storm are due only to soil and groundwater. With groundwater concentration intermediate between the two, the c-Q plot must have lobes that both rise above and dip below the base flow value.

[25] Next, consider the concentration ranking $C_G > C_S > C_E$, the permutation examined in experiment 1. In experiment 2, the first discriminant function for this ranking takes more positive values when event water volume is high, soil water concentration is high, and soil water peak time is early (Table 2, experiment 2). Note that for this concentration ranking, a high soil water concentration reflects a tendency for the soil water to become indistinguishable from the groundwater. Furthermore, with the sequence of peak times constrained to event water—groundwater—soil water, an early soil water peak reflects the same tendency. Therefore a positive discriminant function value for this ranking corresponds to a ''prominent'' event water component, just as it did in experiment 1. Now, however, ''prominent'' refers more generally to the capacity of the event or soil water component, relative to the other, to influence the total concentration. Conversely, when event water volume is small, soil water concentration is low, that is, distinct from groundwater, and the soil water peak is late, that is, also distinct from groundwater, the discriminant function is negative and soil water is prominent. Through a mechanism equivalent to that illustrated for this concentration ranking in experiment 1, a prominent event water component results in an A3 loop, and a prominent soil water component results in a C3 loop (Figure 4 and Table 2, experiment 2). An analogous interpretation applies to the C2 and A2 loops associated with ranking $C_E > C_S > C_G$ (Table 2, experiment 2).

[26] For concentration ranking $C_S > C_E > C_G$, the first discriminant function takes on positive values when the event water peak is late and event water volume is small, and when the soil water peak is late. This corresponds to a situation where event water is relatively indistinguishable from groundwater, and soil water is relatively distinguishable; that is, soil water is prominent (Table 2, experiment 2). When this is the case, the enrichment of total concentration due to soil water on the receding limb exceeds that due to event water on the rising limb, resulting in the ''expected'' A2 loop (Figure 5a). As event water becomes prominent, total concentrations increase along part of the rising limb and decrease along the receding limb, resulting in an indeterminate loop (Figure 5b). An analogous interpretation applies to the C3 and indeterminate loops associated with ranking $C_G > C_E > C_S$ (Table 2, experiment 2).

[27] Note that complete reversal of rotation direction occurs much less frequently for the cases where soil water is at one end of the concentration ranking ($C_S > C_E > C_G$ and $C_G > C_E > C_S$) than for those where soil water is intermediate in the ranking ($C_G > C_S > C_E$ and $C_E > C_S > C_G$) (Table 2, experiment 2). This result is due to the geometry of the component hydrograph layout and the constraints imposed on the range of parameter variation. Soil water is always volumetrically dominant compared to event water (Figure 2). Furthermore, the soil water component has a longer time base, and the range of positions permitted to the two components is such that soil water tends to influence total concentrations over the entire receding limb, whereas event water influences concentrations over only a portion of the rising limb. Thus, when soil water is at one extreme in the ranking, only rare combinations of conditions will cause event water to become sufficiently prominent to completely reverse the rotational direction (Table 2, experiment 2). Therefore, under the conditions imposed in experiment 2, ''expected'' loop types associated with soil water on either end of the concentration ranking tend to be more robust than those with soil water in the middle (Table 2, experiment 2).

4.3. Experiment 3

[28] When mean component concentrations are separated by orders of magnitude, loop types C2 and A2, associated

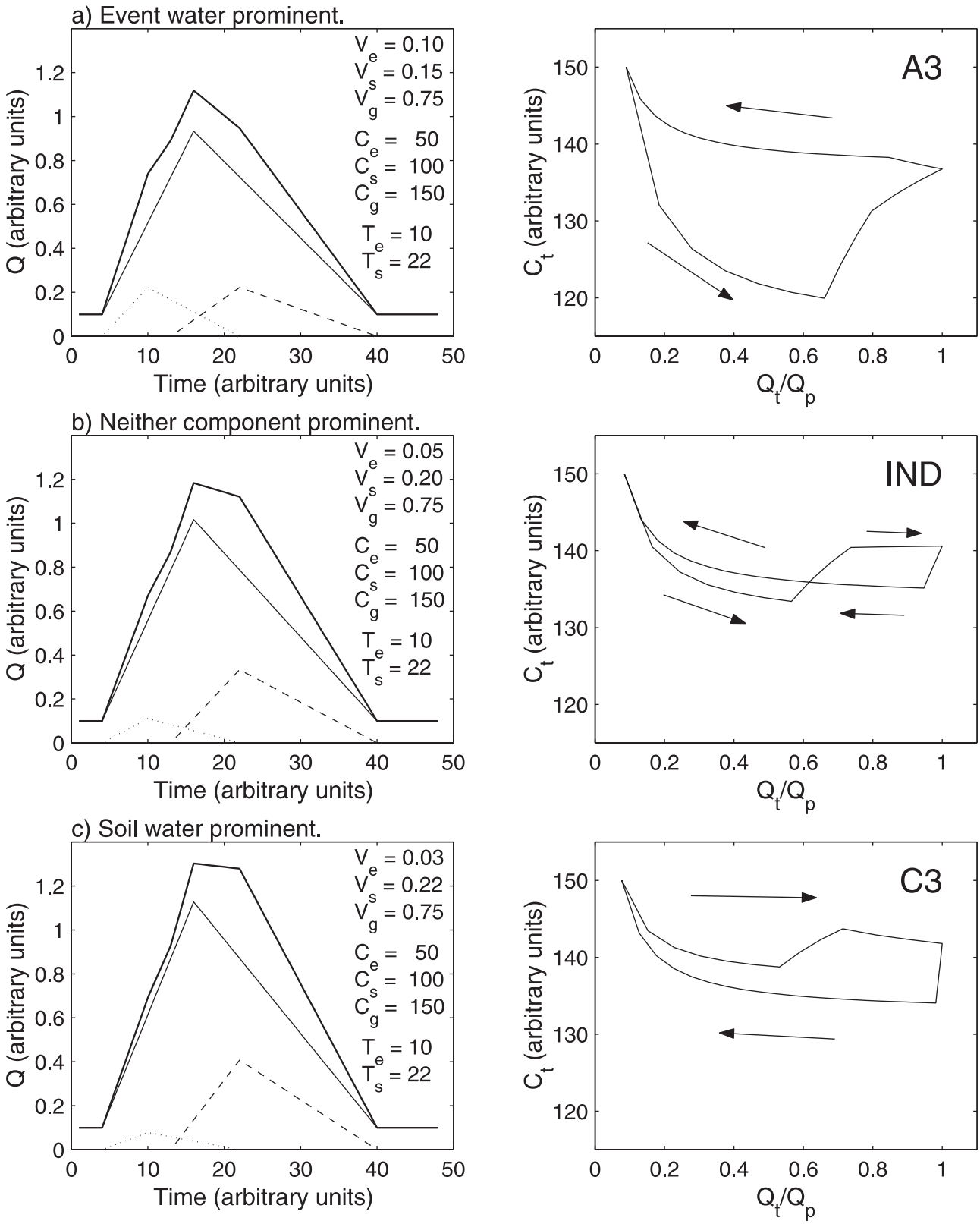

Figure 4. Example of variability in the shapes of loops associated with concentration ranking $C_G > C_S > C_E$ due to variability in relative volume of event and soil water end-members. Arrows indicate direction of rotation. Volume parameters are expressed as a percentage of total storm flow. Refer to section 4.1 for explanation.

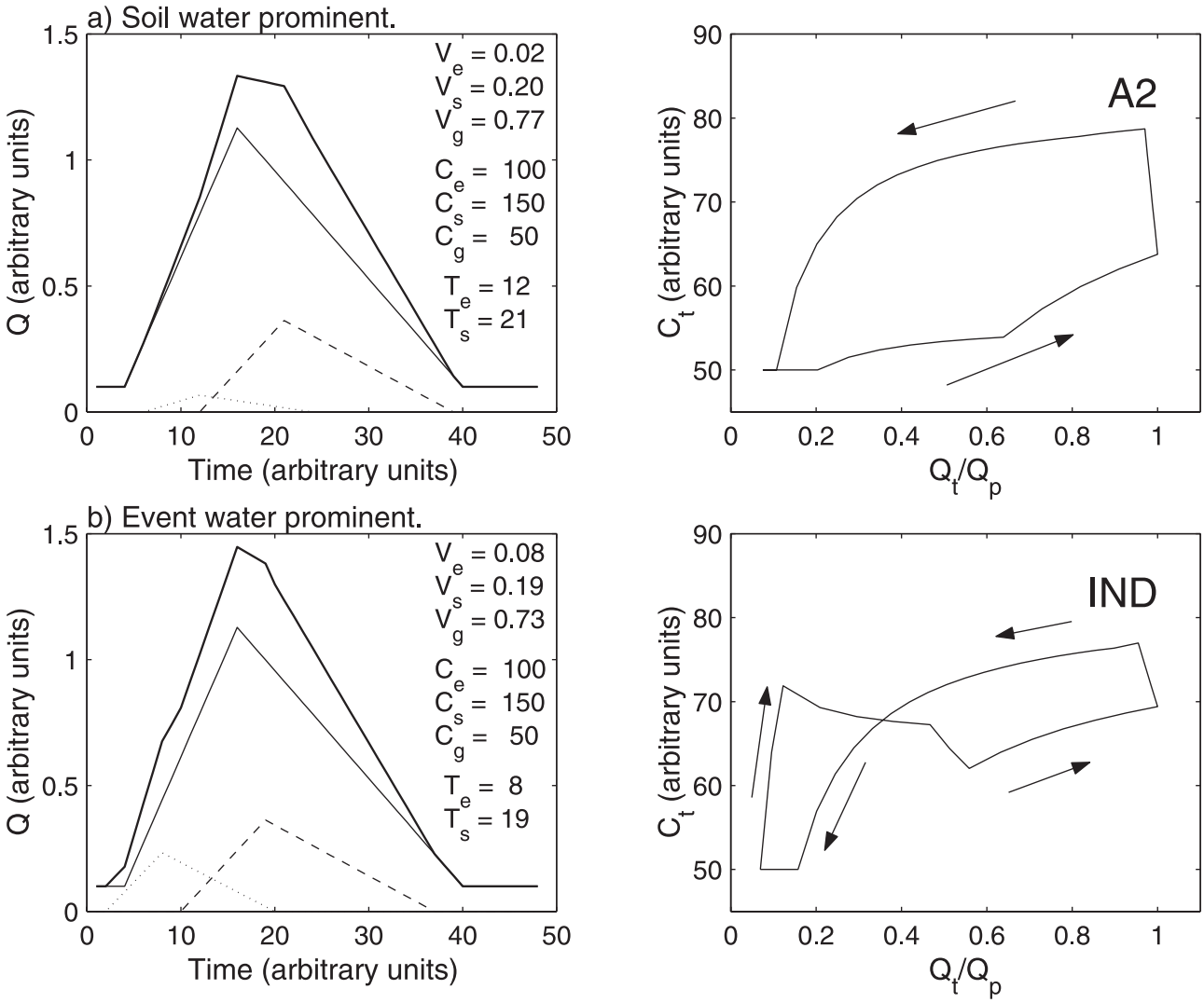

Figure 5. Example of variability in the shapes of loops associated with concentration ranking $C_S > C_E > C_G$ due to variability in volume and timing of event and soil water end-members. Arrows indicate direction of rotation. Volume parameters are expressed as a percentage of total storm flow. Refer to section 4.2 for explanation.

with concentration rankings $C_E > C_S > C_G$ and $C_S > C_E > C_G$, respectively, became more robust than when mean concentrations all lie within the same order of magnitude (Table 2, experiments 2 and 3). In contrast, loop types C3 and A3, associated with rankings $C_G > C_E > C_S$ and $C_G > C_S > C_E$, became less robust. This response may be interpreted by recalling that the "prominence" of the event or soil water components depends on concentration as well as volume and timing. With concentrations so widely separated, they tend to overshadow variability in volume and timing to control the prominence of the hydrograph component to which they are assigned. Therefore "expected" loop types that were favored by a prominent event water component in experiment 2 became more robust when the concentration ranking favored the event water component, and less robust when the ranking favored the soil water component. Conversely, "expected" loop types that were favored by a prominent soil water component in experiment 2 became more robust when the concentration ranking favored the soil water component, and less robust when the ranking favored the event water component (Table 2, experiments 2 and 3).

5. Conclusions

1. Reasonably foreseeable storm-to-storm variability in end-member volume, timing, and concentration can result in several types of loops for a given rank order of concentrations.

2. Concentration rankings $C_E > C_G > C_S$ and $C_S > C_G > C_E$ are always uniquely associated with C1 and A1 loops, respectively. The other four concentration rankings are ambiguously associated with loops that have the same general shape, but which may rotate in either direction.

3. In the ambiguous cases, the rotation direction depends on the relative prominence of the event and soil water end-members in the composite hydrograph. This prominence is broadly defined as a capacity to influence the total concentration, and may result from a combination of end-member volume, timing, or concentration.

4. To the degree that the relative prominence of event and soil water end-members varies continuously, indeterminate loop shapes should be expected.

5. Because of 1–4, inferences of runoff processes based on c-Q plots are strongest when additional information about the prominent hydrograph component and the end-member solute concentrations is available.

[29] **Acknowledgments.** This work was completed under National Science Foundation grant number EAR-9902945. The National Park Service provided additional funding. We gratefully acknowledge the support of both of these agencies. We also thank Ken Hyer, Richard Vogel, Danny Welsch, and two anonymous reviewers for their thoughtful comments on an earlier version of the manuscript.

References

Bazemore, D. E., K. N. Eshleman, and K. J. Hollenback, The role of soil water in stormflow generation in a forested headwater catchment: Synthesis of natural tracer and hydrometric evidence, *J. Hydrol.*, *162*, 47–75, 1994.

Biron, P. M., G. R. Andre, F. Courschesne, W. H. Hendershot, B. Cote, and J. Fyles, The effects of antecedent moisture conditions on the relationship of hydrology to hydrochemistry in a small forested watershed, *Hydrol. Processes*, *13*, 1521–1555, 1999.

Buttle, J. M., Isotope hydrograph separations and rapid delivery of pre-event water from drainage basins, *Prog. Phys. Geogr.*, *18*, 16–41, 1994.

Buttle, J. M., and D. L. Peters, Inferring hydrological processes in a temperate basin using isotopic and geochemical hydrograph separation: A re-evaluation, *Hydrol. Processes*, *11*, 557–573, 1997.

DeWalle, D. R., B. R. Swistock, and W. E. Sharpe, Three-component tracer model for stormflow on a small Appalachian forested catchment, *J. Hydrol.*, *104*, 301–310, 1988.

Evans, C., and T. D. Davies, Causes of concentration/discharge hysteresis and its potential as a tool for the analysis of episode hydrochemistry, *Water Resour. Res.*, *34*, 129–137, 1998.

Evans, C., T. D. Davies, and P. S. Murdoch, Component flow processes at four streams in the Catskill Mountains, New York, analyzed using episodic concentration/discharge relationships, *Hydrol. Processes*, *13*, 563–575, 1999.

Hornberger, G. M., T. M. Scanlon, and J. P. Raffensberger, Modelling transport of dissolved silica in a forested headwater catchment: The effect of hydrological and chemical time scales on hysteresis in the concentration-discharge relationship, *Hydrol. Processes*, *15*, 2029–2038, 2001.

McDonnell, J. J., M. Bonell, M. K. Stewart, and A. J. Pearce, Deuterium variations in storm rainfall: Implications for stream hydrograph separation, *Water Resour. Res.*, *26*, 455–458, 1990.

McDonnell, J. J., M. K. Stewart, and I. F. Owens, Effect of catchment-scale subsurface mixing on stream isotopic response, *Water Resour. Res.*, *27*, 3065–3073, 1991.

Pionke, H. B., and D. R. DeWalle, Intrastorm and interstorm O-18 trends for selected rainstorms in Pennsylvania, *J. Hydrol.*, *138*, 131–143, 1992.

Scanlon, T. M., J. P. Raffensperger, and G. M. Hornberger, Modeling transport of dissolved silica in a forested headwater catchment: Implications for defining the hydrochemical response of observed flow pathways, *Water Resour. Res.*, *37*, 1071–1082, 2001.

Swistock, B. R., D. R. DeWalle, and W. E. Sharpe, Sources of acidic stormflow in an Appalachian headwater stream, *Water Resour. Res.*, *25*, 2139–2147, 1989.

J. G. Chanat and G. M. Hornberger, Department of Environmental Sciences, University of Virginia, Charlottesville, VA 22903, USA. (jgc3n@virginia.edu)

K. C. Rice, U.S. Geological Survey, Charlottesville, VA 22903, USA.